

available at www.sciencedirect.comwww.elsevier.com/locate/brainres**BRAIN
RESEARCH**

Research Report

Neuroanatomical changes due to hearing loss and chronic tinnitus: A combined VBM and DTI study

Fatima T. Husain^{a,b,*}, Roberto E. Medina^a, Caroline W. Davis^a, Yvonne Szymko-Bennett^b,
Kristina Simonyan^c, Nathan M. Pajor^b, Barry Horwitz^b

^aDepartment of Speech and Hearing Science, University of Illinois at Urbana-Champaign, Champaign, IL, USA

^bBrain Imaging and Modeling Section, National Institute on Deafness and Other Communication Disorders, National Institutes of Health, Bethesda, MD, USA

^cLaryngeal and Speech Section, National Institute of Neurological Disorders and Stroke, National Institutes of Health, Bethesda, MD, USA

ARTICLE INFO

Article history:

Accepted 26 October 2010

Available online 1 November 2010

Keywords:

Voxel-based morphometry

VBM

Diffusion tensor imaging

DTI

MRI

Brain

Structure

Tinnitus

Hearing loss

Hearing impairment

Gray matter

Grey matter

White matter

ABSTRACT

Subjective tinnitus is the perception of sound in the absence of an external source. Tinnitus is often accompanied by hearing loss but not everyone with hearing loss experiences tinnitus. We examined neuroanatomical alterations associated with hearing loss and tinnitus in three groups of subjects: those with hearing loss with tinnitus, those with hearing loss without tinnitus and normal hearing controls without tinnitus. To examine changes in gray matter we used structural MRI scans and voxel-based morphometry (VBM) and to identify changes in white matter tract orientation we used diffusion tensor imaging (DTI). A major finding of our study was that there were both gray and white matter changes in the vicinity of the auditory cortex for subjects with hearing loss alone relative to those with tinnitus and those with normal hearing. We did not find significant changes in gray or white matter in subjects with tinnitus and hearing loss compared to normal hearing controls. VBM analysis revealed that individuals with hearing loss without tinnitus had gray matter decreases in anterior cingulate and superior and medial frontal gyri relative to those with hearing loss and tinnitus. Region-of-interest analysis revealed additional decreases in superior temporal gyrus for the hearing loss group compared to the tinnitus group. Investigating effects of hearing loss alone, we found gray matter decreases in superior and medial frontal gyri in participants with hearing loss compared to normal hearing controls. DTI analysis showed decreases in fractional anisotropy values in the right superior and inferior longitudinal fasciculi, corticospinal tract, inferior fronto-occipital tract, superior occipital fasciculus, and anterior thalamic radiation for the hearing loss group relative to normal hearing controls. In attempting to dissociate the effect of tinnitus from hearing loss, we observed that hearing loss rather than tinnitus had the greatest influence on gray and white matter alterations.

© 2010 Elsevier B.V. All rights reserved.

* Corresponding author. Department of Speech and Hearing Science, University of Illinois at Urbana-Champaign, 901 S. Sixth Street, MC-482, Champaign, IL 61820. Fax.: +1 217 244 2235.

E-mail address: husainf@illinois.edu (F.T. Husain).

Abbreviations: VBM, voxel-based morphometry; MRI, magnetic resonance imaging; DTI, Diffusion Tensor Imaging; FA, fractional anisotropy; ROI, region-of-interest; SPM, statistical parametric mapping; FSL, FMRIB software library

1. Introduction

Tinnitus, from the Latin word *tinnire* for “to ring,” is a phantom perception of sound when no such sound is present externally. Although most incidences of tinnitus are temporary, chronic subjective tinnitus occurs in 4–15% of the general population, with the prevalence increasing in those above 50 years of age to almost 20% (Moller, 2007). Broadly speaking, about 90% of individuals with chronic tinnitus have some form of hearing loss; however, only about 30–40% of those with hearing loss develop tinnitus (Davis and Rafaie, 2000; Lockwood et al., 2002; Moller, 2007). For instance, Barnea et al. (1990) found that 8% of patients with tinnitus had normal hearing thresholds (defined as better than or equal to 20 dB HL) up to 8000 Hz. As reported by the National Center for Health Statistics (Adams et al., 1999) tinnitus affects about 12% of the men between the ages of 65–74 years and the prevalence of hearing impairment in the tinnitus population is between 80 and 90%. Hearing loss affects about 35% of men between the ages of 65–74 years. This means, approximately 65–70% of those with hearing loss in the 65–75 years range do not suffer from tinnitus. The prevalence of hearing loss is lower in the 45–64 years range; however, the percentage of those with tinnitus in the hearing impaired group is similar. Although there have been several brain imaging studies investigating neural bases of tinnitus, few have examined its relationship with hearing loss, and the exact mechanisms and brain regions associated with tinnitus remain poorly understood. In the present study, we investigated structural gray and white matter changes related to tinnitus and hearing loss and attempted to dissociate them from changes due to hearing loss alone. Spatial patterns of structural change are a means of studying long-term functional changes associated with chronic tinnitus or hearing loss and are indicative of potential mechanisms causing such changes. We used voxel-based morphometry (VBM) to compare the volume and concentration of gray matter between tinnitus and non-tinnitus groups at the voxel-level using high-resolution magnetic resonance imaging (MRI). Further, we used diffusion tensor imaging (DTI) to investigate changes in organization of white matter tracts between tinnitus and non-tinnitus groups.

Functional brain imaging studies in humans have provided evidence for a distributed network of cortical regions associated with tinnitus (Giraud et al., 1999; Lockwood et al., 2001; Lockwood et al., 2002; Mirz et al., 2000a,b; Smits et al., 2007). There have been three studies to date investigating the gross anatomical changes in gray matter in individuals with tinnitus (Landgrebe et al., 2009; Muhlau et al., 2006; Schneider et al., 2009). The previous studies using VBM (Landgrebe et al., 2009; Muhlau et al., 2006) provide evidence for gray matter changes in individuals with tinnitus and normal hearing relative to a normal hearing non-tinnitus control group in both the auditory and limbic systems. The specific structures within these systems identified by the two studies are different. Muhlau et al. found gray matter increases in the thalamus and gray matter decreases in the subcallosal frontal cortex, while Landgrebe and colleagues detected gray matter decreases in the right inferior colliculus and the left hippocampus for the tinnitus participants relative to controls. Whereas the thala-

mus and inferior colliculus are prominent and necessary junctures in the central auditory system, subcallosal frontal cortex and the hippocampus are associated with processing of emotion and memory, respectively, and are part of the limbic system. The patient demographics in both studies were similar. However, there may be other contributory factors for the different results: there were some differences in the patient characteristics related to laterality of perceived tinnitus (majority in both studies perceived the tinnitus as bilateral, a minority perceived it as lateralized) and personality traits or depressive symptoms (8 patients had mild-to-moderate depressive symptoms in the Landgrebe study but not in the Muhlau study). Therefore, although these studies are informative, they present contradictory results and cannot necessarily be generalized to the larger tinnitus population with hearing loss. In contrast, Schneider et al. (2009)'s study included those with hearing loss in addition to tinnitus. Using individual morphological segmentation, Schneider et al. (2009) found gray matter reductions in medial Heschl's gyrus for those with tinnitus relative to controls without tinnitus (29 out of the 42 control participants had normal hearing). The study also found some evidence for an association between volume reduction and hearing loss, dependent on the tinnitus status, musical training of the participant and the degree of symmetry of their hearing loss. The study concentrated on Heschl's gyrus and did not include non-primary auditory cortex regions in its investigation. Thus, there remains the outstanding question about the extent and type of gray matter changes in the auditory and non-auditory processing areas due to hearing loss and tinnitus.

Animal studies, much like human studies, have mainly focused on the functional consequences of hearing loss or tinnitus along the central auditory processing pathway. These studies have implicated physiological changes in the dorsal cochlear nucleus (Kaltenbach et al., 2000), the inferior colliculus (Chen and Jastreboff, 1995; Wang et al., 2002), thalamus (Basta et al., 2005; Basta et al., 2008), and the auditory cortices (Basta et al., 2008; Eggermont and Kenmochi, 1998). A few animal studies investigating structural changes after hearing loss found reduced cell density in the brain stem, specifically in the dorsal cochlear nucleus, superior olive and the inferior colliculus (Kim et al., 1997), and medial geniculate body of the thalamus and the primary auditory cortex (Basta et al., 2005).

The first study to investigate white matter microstructural integrity in persons with tinnitus was a pilot study (Lee et al., 2007), but there have been other DTI investigations focused on sensorineural hearing loss (Chang et al., 2004; Lee et al., 2004; Lin et al., 2008). Chang et al. (2004) focused their attention on the central auditory pathways, primarily in the brainstem region, by performing partial-brain diffusion tensor imaging and doing a further focused region-of-interest analysis. They found significantly reduced fractional anisotropy (FA) values for participants with hearing loss in the fiber tracts passing through the superior olivary nucleus, lateral lemniscus, inferior colliculus and auditory radiation regions. FA is a measure of the degree of diffusion directionality, and is sensitive to changes in white matter microstructure; a large FA value implies that white matter tracts are oriented in the same direction and a lower FA value indicates loss of white matter or that white matter tracts are disorganized and

radiating in all directions. The subjects were of both genders, ranged in age from 8 to 85 years with mild-to-severe hearing loss and 2 of the 10 subjects had unilateral hearing loss while the remaining 8 had bilateral hearing loss. The heterogeneity of the subject population severely limits interpretation and generalization of the study. Lin et al. (2008) studied three groups of patients: those with bilateral hearing loss, those with unilateral hearing loss and those with partial hearing loss. They focused their investigation on two ROIs in the lateral lemniscus and the inferior colliculus where they found decreased FA values for all patients. This suggests that hearing loss may be associated with uniform changes in white matter orientation; however, it is not clear how such changes will occur when hearing loss is accompanied by chronic tinnitus, and whether such white matter changes occur in other brain areas, particularly in neocortex.

The intent of the present study was to investigate the effect of chronic tinnitus and hearing loss on the brain's gross anatomy and dissociate these changes from those due to hearing loss alone. Our specific focus was the region around the primary auditory cortex and auditory processing pathways, leading into and out of the primary auditory cortex. Our hypothesis was that there are distinct spatial patterns of gray and white matter changes that are related to hearing loss or tinnitus. Based on previous studies, we expected that there are tinnitus-related volumetric changes in gray matter in inferior colliculus, parts of the thalamus, and subcallosal frontal cortex. Based on previous DTI studies of sensorineural hearing loss, we expected changes in orientation of subcortical white matter tracts in the anterior thalamic radiation and lateral lemniscus.

2. Results

Three groups of subjects participated in the study: TIN (those with tinnitus and hearing loss), HL (those with hearing loss without tinnitus), and NH (normal hearing individuals without tinnitus). We conducted a structural MRI study to investigate both changes in gray matter using VBM and in white matter using DTI.

2.1. VBM

We conducted unbiased whole-brain and two region-of-interest (ROI) analyses of the modulated (indicative of volume) and unmodulated (indicative of concentration) VBM data. The first ROI analysis was based on *a priori* hypotheses regarding central auditory processing brain regions showing involvement in tinnitus perception and previously used by Landgrebe et al. (2009) and Muhlau et al. (2006). The second ROI analysis was similar, but it included a mask of significant brain regions from our whole-brain group comparisons and the patients' pure tone average (PTA) hearing loss estimate as an imaging covariate. The whole-brain ANOVA analysis of modulated VBM data showed a main effect of group, with the suprathreshold voxels being in anterior cingulate gyrus, medial frontal gyrus, and superior frontal gyrus. However, the whole-brain analysis of unmodulated VBM data did not show any statistically significant main effect of group and we did not include these data in our report. In all cases of whole-brain analysis, the results of the non-parametric SnPM examinations corroborated the results of the conventional SPM analysis. Here, we report only results from the SPM analysis. To

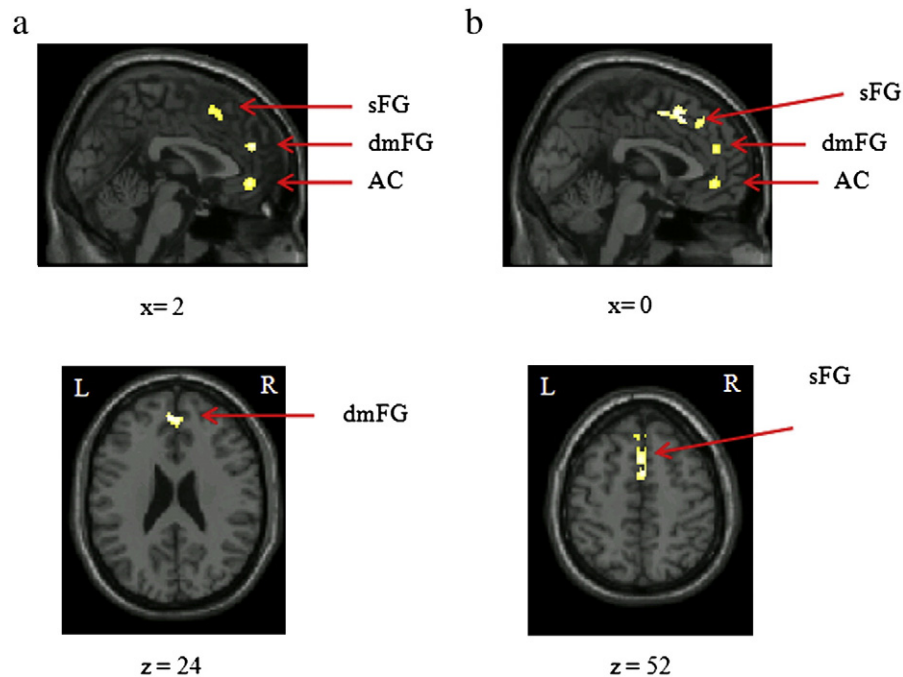


Fig. 1 – Statistical parametric maps of whole-brain VBM analyses displayed on a template brain. (a) Gray matter decreases in hearing loss compared to normal hearing controls (HL < NH) in volume. (b) Gray matter decreases in hearing loss alone compared to hearing loss and tinnitus (HL < TIN) in volume and concentration, respectively. The threshold was $p < 0.05$ corrected for multiple comparisons at voxel and cluster level, extent threshold of 50 contiguous voxels.

answer our specific questions, we performed two-sample *t* tests on pairs of groups to test for gray matter changes in modulated.

- (1) **HL vs. NH:** Whole-brain analysis of modulated (volume) data showed decreases for HL relative to NH in right anterior cingulate and bilateral medial frontal gyrus (see Fig. 1 and Table 2). We did not find any suprathreshold voxels for the NH<HL contrast in the whole-brain analysis. Our first ROI analysis showed significant gray matter volume declines in bilateral superior temporal gyrus for HL relative to NH participants (see Fig. 2 and Table 2). A subsequent ROI analysis with pure tone average hearing loss as a covariate using a combined mask of the auditory ROIs and the group comparison local maxima revealed significant volumetric decreases in the superior and medial frontal gyri for NH>HL contrast that were associated with hearing loss (see Fig. 3a and Table 2).
- (2) **TIN vs. HL:** Whole-brain analysis of modulated data for the HL<TIN contrast showed significant gray matter decreases in bilateral superior frontal gyrus, and bilateral medial frontal gyrus for HL relative to the TIN group (see Fig. 1 and Table 2). We did not find any suprathreshold voxels for the TIN<HL contrast in the whole-brain analysis. ROI analysis revealed gray matter volume decreases for HL compared to the TIN group in bilateral superior temporal gyrus (see Fig. 2 and Table 2). A subsequent analysis with pure tone average hearing loss as a covariate using both a combined mask of the ROIs and the group comparison local maxima revealed significant volumetric decreases in the central superior and medial frontal gyri for the TIN>HL contrast that were associated with hearing loss (see Fig. 3b and Table 2).
- (3) **TIN vs. NH:** We found no significant gray matter disparities of volume or concentration for the tinnitus group relative to the normal hearing controls using either the whole-brain or the ROI analysis. We could not confirm gray matter decreases in the subcallosal frontal cortex (Muhlau et al., 2006) or the right inferior colliculus and left hippocampus (Landgrebe et al., 2009) as reported earlier, nor did we detect gray matter increases in the right posterior thalamus (Muhlau et al., 2006) in tinnitus patients as compared to normal hearing controls. There are differences in the cluster sizes between our study and the Muhlau study, although, the Z-scores of the clusters having peak voxels in our study were within the range of the other studies (Muhlau et al., 4.9 max and 3.7 min; Landgrebe et al., 4.49 max and 4.28 min; our study 4.18 max, and

3.04 min). The Muhlau study found larger clusters of 5234 (whole-brain) and 388 (ROI) voxels while our clusters averaged 94 voxels for the whole-brain analysis and 127 voxels for the ROI analysis. The Landgrebe study does not provide information about their cluster sizes. Whereas cluster size could be affected by the number of scans analyzed, it varies largely across VBM studies reflecting mainly the results of local smoothing in non-stationary data. Larger clusters appear in areas where the images are very smooth and smaller clusters in comparatively very rough areas.

2.2. DTI

Unbiased whole-brain TBSS analysis (Tract-based Spatial Statistics, Smith et al., 2006) was used to obtain FA values for each of the three groups. The whole-brain significant group comparison results for the FA values are shown in Fig. 4 and Table 3. We found significant differences in the FA values for the NH>HL contrast alone; results from other group comparisons did not reach statistical significance. Clusters showing a decrease in FA values for hearing loss subjects compared to normal hearing controls were found in one large cluster of tracts that comprised the corticospinal tract (part of superior corona radiata), inferior and superior longitudinal fasciculi, inferior fronto-occipital fasciculus, superior occipital fasciculus and anterior thalamic radiations (specifically acoustic radiation), all in the right hemisphere. No significant differences in white matter FA values were observed on the left side of the brain.

We performed two other analyses. In the first one, we used the PTA hearing loss estimate as a covariate in the group comparisons, specifically, that of NH vs. HL that showed significant results in the whole-brain analysis. We found statistically significant voxels in the right anterior thalamic radiation, inferior fronto-occipital fasciculus and inferior longitudinal fasciculus for the NH>HL comparison (Fig. 5a). Using this cluster, we performed a second ROI analysis at a lower significance threshold to explore differences between the three groups. We computed FA values for each subject within an ellipsoid ROI drawn in the right hemispheres (see Fig. 5b for the ROI). The left hemispheric ROI did not show significant differences in any of the group-wise comparisons; therefore, data from the left ROI are not reported. Both hearing loss groups (with and without tinnitus) showed lower FA values relative to normal hearing controls in the right anterior thalamic radiation, inferior fronto-occipital fasciculus and inferior longitudinal fasciculus. This was highly significant for

Table 1 – Average hearing thresholds of test participants. NH=normal hearing, HL=hearing loss and TIN=hearing loss accompanied by tinnitus.

| | Frequency (Hz) | | | | | | | |
|-----------|----------------|----------|----------|-----------|-----------|-----------|-----------|-----------|
| | 250 | 500 | 1000 | 2000 | 3000 | 4000 | 6000 | 8000 |
| TIN (n=8) | 11.3±9.0 | 10.9±8.4 | 13.8±7.6 | 18.1±10.5 | 30.9±18.1 | 42.5±18.3 | 48.1±15.7 | 45.6±17.1 |
| HL (n=7) | 13.1±4.4 | 12.8±4.1 | 13.8±6.5 | 20.3±13.0 | 28.8±19.0 | 32.8±18.8 | 40.0±17.0 | 41.6±17.0 |
| NH (n=11) | 6.6±3.6 | 7.0±4.0 | 8.0±4.8 | 9.3±5.6 | 11.8±5.7 | 14.1±7.8 | 20.2±5.7 | 16.8±8.5 |

Thresholds in dB HL (± 1SE) were obtained using standard clinical procedures.

Table 2 – Local maxima from the different contrasts highlighting gray matter differences between the groups, obtained using VBM analysis. The statistical thresholds and contrasts are indicated within the table.

| | Coordinates | | | Significance | | | Score | Cluster size (k) |
|---|-------------|-----|----|----------------------------------|--------------------------------|---------------|-------|------------------|
| | MNI | | | p FWE corrected at cluster level | p FDR corrected at voxel-level | p uncorrected | Z | Voxels |
| <i>(1) Whole-brain one-way ANOVA: main effect of group p<0.001 uncorrected. k=50</i> | | | | | | | | |
| Superior Frontal Gyrus Center, Right. | 0 | 16 | 52 | - | .241 | .000 | 3.86 | 180 |
| | 2 | 4 | 54 | | | | | |
| Medial Frontal Gyrus Bilateral | -4 | 48 | 24 | - | .241 | .000 | 3.84 | 103 |
| | 2 | 44 | -6 | | | | 3.75 | 71 |
| Cingulate Gyrus | 2 | 32 | 48 | - | .241 | .000 | 3.35 | 60 |
| <i>(2) Group analysis Two-sample t tests masked by ANOVA results, p<0.05 FWE corrected at the cluster and voxel levels. k=50</i> | | | | | | | | |
| <i>HL<TIN</i> | | | | | | | | |
| Superior Frontal Gyrus Bilateral | 0 | 16 | 52 | .001 | .000 | .000 | 4.18 | 180 |
| | 2 | 4 | 54 | | | | | |
| | -2 | 28 | 48 | | | | | |
| Medial Frontal Gyrus Bilateral | -4 | 46 | 24 | .001 | .000 | .000 | 3.98 | 102 |
| | 2 | 44 | -6 | | | | 3.97 | 71 |
| <i>HL<NH</i> | | | | | | | | |
| Medial Frontal Gyrus Bilateral | 2 | 46 | 24 | .001 | .001 | .000 | 3.94 | 79 |
| | 2 | 44 | -6 | .002 | | | 3.71 | 67 |
| | -2 | 46 | 4 | .002 | | | 3.37 | 67 |
| Anterior Cingulate Right | 2 | 20 | 48 | .001 | .001 | .000 | 3.48 | 93 |
| Superior Frontal Gyrus Left | -2 | 16 | 54 | .001 | .001 | .000 | 3.48 | 93 |
| <i>(3) ROI analysis</i> | | | | | | | | |
| <i>3.1 Auditory Mask (Muhlau), p<0.005 Uncorrected k=20</i> | | | | | | | | |
| <i>HL<TIN</i> | | | | | | | | |
| Superior Temporal Gyrus Bilateral | 58 | 10 | -6 | .725 | .001 | .001 | 3.04 | 267 |
| | -66 | -30 | 16 | .796 | .236 | .003 | 2.70 | 70 |
| <i>HL<NH</i> | | | | | | | | |
| Superior Temporal Gyrus Bilateral | -60 | 2 | 4 | .998 | .044 | .000 | 4.01 | 27 |
| | 62 | 2 | 4 | .986 | .178 | .001 | 3.25 | 68 |
| <i>3.2 (ANOVA mask(1)+auditory mask (Muhlau) with PTA as a regressor, p<0.001 uncorrected, p≤.005 FWE corrected at the cluster level. k=50</i> | | | | | | | | |
| <i>HL<TIN</i> | | | | | | | | |
| Superior Frontal Gyrus Center, Right | 0 | 16 | 54 | .013 | .028 | .000 | 3.73 | 132 |
| | 2 | 2 | 54 | | | | 3.66 | |
| Medial Frontal Gyrus Bilateral | -6 | 50 | 28 | .055 | .028 | .000 | 3.64 | 81 |
| | 2 | 46 | 22 | | | | 3.54 | |
| <i>HL<NH</i> | | | | | | | | |
| Medial Frontal Gyrus Bilateral | 2 | 12 | 52 | .001 | .024 | .000 | 4.16 | 270 |
| | -4 | 48 | 24 | | | | 3.87 | 120 |
| Anterior Cingulate Left | -4 | 54 | 30 | .018 | .024 | .000 | 3.54 | 120 |
| Superior Frontal Gyrus Left | -4 | 54 | 30 | .018 | .024 | .000 | 3.54 | 120 |

normal hearing controls compared to the hearing loss group without tinnitus ($p=0.0006$ using Wilcoxon rank sum test) and less so for normal hearing controls compared to the tinnitus group ($p=0.014$ using Wilcoxon rank sum test). Hearing loss subjects showed the largest decrease in FA values, while those with tinnitus had FA values intermediate to those between hearing loss and normal hearing subject groups. Although there was a trend, there were no statistically significant differences in the FA values of those with tinnitus and those without tinnitus but with hearing loss ($p=0.07$ using Wilcoxon rank sum test). We also tested for the effect of hearing loss, regardless of tinnitus status. We found that the FA values of the normal hearing group in this region were significantly

higher than for the combined hearing loss groups, regardless of the tinnitus status ($p=0.001$ using Wilcoxon rank sum test).

In order to understand the relative differences between HL and TIN FA values, we plotted the FA values of the three groups for the right ROI against PTA HL values at 2,4,6,8 kHz PTA (5c). Fig. 5 shows the relationship between FA values and degree of hearing loss in the first case for the three groups. We found that both hearing loss groups had lower FA values compared to the normal hearing controls, with some of the FA values of the TIN group being more intermediate. The TIN group had intermediate values even though they had a similar degree of hearing loss as the HL group. This may partially explain the difference in significance in the NH>HL versus the

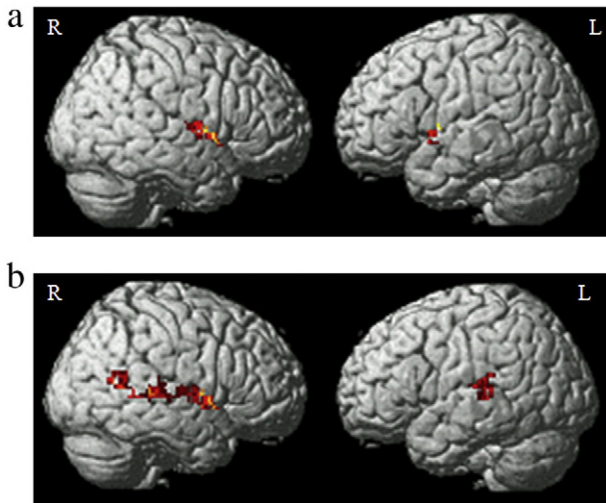


Fig. 2 – Statistical parametric maps of ROI analysis of VBM data rendered on a template brain image, showing gray matter declines in (a) HL<NH and (b) HL<TIN contrasts. The threshold was set at $p < 0.005$ uncorrected and extent threshold of 20 contiguous voxels.

NH>TIN comparisons. None of the correlations between FA and PTA values for any group was significant.

2.3. Combined VBM-DTI results

Fig. 6 depicts both FA and VBM values for the NH>HL contrast that showed the most significant results. The FA values (blue color) showed greatest declines in the inferior fronto-occipital fasciculus, inferior and superior longitudinal fasciculi and anterior thalamic radiation, representing loss of white matter microstructure integrity, for the HL group relative to the normal hearing controls. The superior longitudinal and fronto-occipital fasciculi connect frontal cortex with posterior parts of the cortex. The greatest reductions in gray matter volume (green color) for the same comparison were observed in the frontal cortex: superior and medial frontal gyri. We also

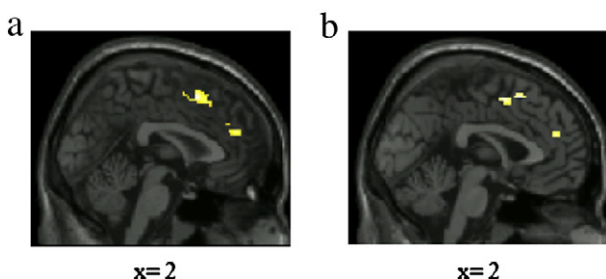


Fig. 3 – Effect of hearing loss on gray matter. Statistical parametric maps of multiple regression analysis with the PTA hearing loss as a covariate for the VBM dataset. (a) HL<NH (volume decreases in HL, $x=2$), (b) HL<TIN (volume decreases in HL, $x=2$). The threshold was set at $p < 0.001$ uncorrected at voxel-level and $p < 0.05$ FWE correct at cluster level with an extent threshold of 20 contiguous voxels.

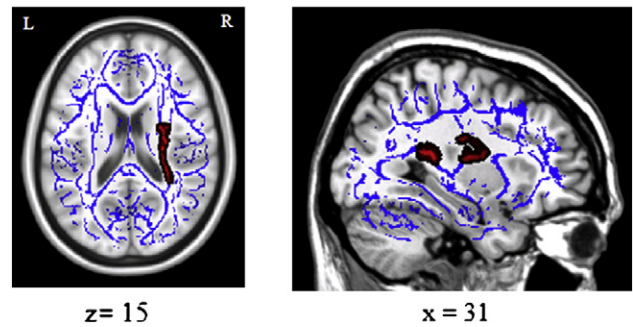


Fig. 4 – Whole-brain group comparisons (HL<NH) of DTI data obtained using tract-based spatial statistics of FSL (corrected for multiple comparisons at $p < 0.1$ using permutation-based tests). The statistically significant clusters are depicted in red color over a FA skeleton map in blue color. Only the HL<NH comparison was significant. Shown is an axial slice at $z=17$ and a sagittal slice at $x=31$.

plotted the results of the ROI VBM analysis (red color) in the superior temporal gyrus. The anterior thalamic radiation and the inferior fronto-occipital fasciculus, both of which showed declines in FA values for the HL group (relative to the NH controls), connect to and from the superior temporal gyrus.

3. Discussion

Subjective tinnitus occurs frequently as a consequence of hearing impairment. The hearing loss can cause reorganization of the auditory nerve, the central auditory processing pathways and the cortex, possibly leading to tinnitus. However, the underlying neural mechanisms and changes associated with tinnitus are poorly understood and not everyone with hearing loss develops tinnitus. The aim of the present study was to investigate gray and white matter changes in individuals with tinnitus and hearing loss and dissociate the effect of tinnitus from that of hearing loss alone. We conducted both unbiased whole-brain analysis and region-of-interest analysis (based on *a priori* hypotheses) of structural and diffusion MRI data. The most salient result of our study was that neuroanatomical changes (in both gray and white matter) in the vicinity of the auditory cortex were most profound for individuals with hearing loss without tinnitus than individuals with hearing loss and tinnitus when compared to normal hearing controls. Whole-brain analysis revealed gray matter decreases for the hearing loss group in regions distal from the central auditory processing areas, both in comparison with the tinnitus group and the normal hearing control group. Some of these regions, medial frontal gyrus, superior frontal gyrus, and anterior cingulate, are associated with cognitive function and attention, rather than with sensory processing. ROI analysis revealed gray matter decreases in the bilateral superior temporal gyrus (secondary auditory cortex) for those with hearing impairment relative to the TIN and NH groups. DTI whole-brain analysis revealed

Table 3 – Local maxima from the different contrasts highlighting white matter orientation (specified as fractional anisotropy or FA) differences between the groups, obtained using DTI analysis. Correction for multiple comparisons was performed using permutation-based inference with a significance level of $p < 0.1$ and an extent threshold of 15 contiguous voxels.

| Location | Coordinates | | | Cluster size (k) Voxels | $p < 0.001$ unco | $p < 0.1$ corr |
|---|-------------|-----|----|----------------------------|---------------------|-------------------|
| | MNI | | | | | |
| | X | Y | Z | | | |
| (1) NH>HL | | | | | | |
| Inf. Fronto-occipital fasciculus, inf. Longitudinal fasciculus, acoustic radiation (part of thalamic radiation) Right | 32 | -36 | 16 | 851 | 0.001 | 0.061 |
| Corticospinal tract Right | 26 | -15 | 21 | | 0.001 | 0.062 |
| Sup. Occipital Fasciculus, Corticospinal tract Right | 25 | -24 | 22 | | 0.001 | 0.065 |
| Sup. Occipital Fasciculus Right | 21 | -16 | 24 | | 0.001 | 0.066 |
| Corticospinal tract Right | 28 | -13 | 16 | | 0.001 | 0.069 |
| Inf. Fronto-occipital fasciculus, inf. Longitudinal fasciculus, ant. Thalamic radiation Right | 31 | -42 | 17 | | 0.001 | 0.076 |
| Sup. Longitudinal Fasciculus Right | 31 | -7 | 15 | | 0.001 | 0.082 |
| (2) NH>HL regression with PTA | | | | | | |
| Inf. Fronto-occipital fasciculus, inf. Longitudinal fasciculus, ant. Thalamic radiation | 30 | -35 | 16 | 28 | 0.001 | 0.1 |

significant differences in orientation of white matter tracts leading into and out of superior temporal cortex and the frontal cortex for the HL group relative to the NH group, but there were no statistically significant differences with the TIN group. Finally, in comparing the tinnitus group

with the normal hearing group, we did not find any statistically significant differences in gray matter size or white matter tract orientation between the two groups. We next discuss separately the results from the VBM and DTI analyses.

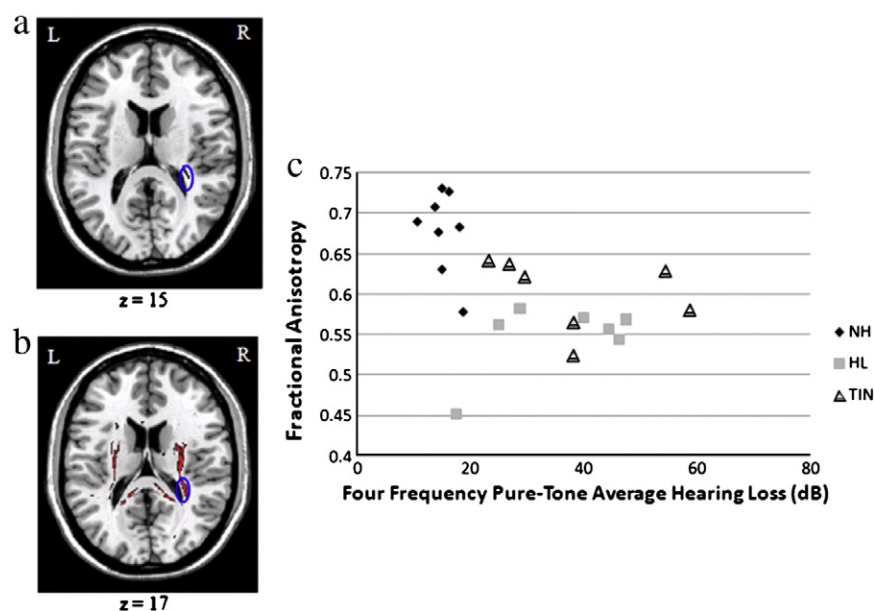


Fig. 5 – Effect of hearing loss on white matter tracts. (a) Significant results of a regression analysis using PTA (2, 4, 6, and 8 kHz) hearing loss estimates a covariate for the HL<NH comparison. The axial slice shown is at $z = 15$. (b) Unthresholded results of HL<NH comparison shown at $z = 17$ with the ROI drawn on the right hemisphere. The ROI was defined as an ellipsoid (with axes dimensions $a = 2$, $b = 5$, $c = 2$) centered on MNI coordinates (31, 37, 16) located in the right anterior thalamic radiation, inferior fronto-occipital fasciculus and inferior longitudinal fasciculus. (c) The FA values within ROI (shown in b) in the white matter tracts near primary auditory cortex are plotted against the PTA values for each participant from each group. See text for details.

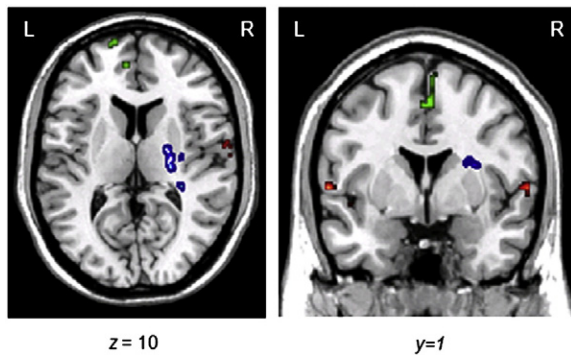


Fig. 6 – Across-group analysis of gray matter volume and white matter FA values for NH>HL comparison revealed reductions in gray matter volume (blue), and FA values (red) at the whole-brain level. In ROI analysis, gray matter volume reductions were found in bilateral superior temporal gyri (green).

3.1. VBM

A major finding of our study is that hearing loss causes gray matter decreases in cortical regions, either associated with auditory or non-auditory processing. To our knowledge, this is the first whole-brain study reporting on gray matter changes due to mild-to-moderate hearing loss. That hearing loss is related to structural changes in the brain is not surprising. Earlier studies have found white matter changes in auditory processing pathways in the brain stem in individuals with sensorineural hearing loss (Chang et al., 2004; Lin et al., 2008). In a larger study of tinnitus patients and non-tinnitus controls, Schneider et al. (2009) found that gray matter declines in the medial Heschl's gyrus were associated with degree of hearing loss, apart from a greater correlation of these reductions with tinnitus. However, studies in congenitally deaf adults did not show differences in gray matter volume in the auditory processing areas (Penhune et al., 2003), although there may be alteration in the white matter in the posterior superior temporal gyrus (Shibata, 2007).

Our results supported some of the results obtained by the Muhlau et al. (2006) and the Landgrebe et al. (2009) studies, but not others. The cluster of gray matter declines in the NH>HL contrast in the subcallosal frontal cortex (peak value of [2, 44, -6], cluster size 71 voxels) falls within the cluster of gray matter decreases in the subcallosal frontal cortex (peak value of [4, 20, -6], cluster size 5234 voxels) for the tinnitus group relative to the normal hearing group found by Muhlau et al. (2006). However, we did not find any alterations in this region for the tinnitus group relative to the non-tinnitus groups. Similar to the results of Landgrebe et al. (2009), we could not replicate the finding of thalamic-level gray matter decreases in TIN relative to NH, observed by Muhlau et al. (2006). We also did not find changes in the inferior colliculus or the hippocampus as reported by Landgrebe et al. (2009). These previous VBM studies of tinnitus (Landgrebe et al., 2009; Muhlau et al., 2006) only included individuals with normal hearing. Our study did not include any tinnitus participant with normal hearing. When we compared tinnitus with hearing loss to the

normal hearing control group, we found no significant differences in concentration or size of gray matter, either in the whole-brain analysis or in the ROI analysis. Therefore, the differences between our study and the previous VBM studies may be due to any of several reasons, including demographic and technical factors. Our study had the additional condition of hearing loss in the tinnitus group, and it also had smaller homogeneous sample size relative to the other two studies. All of our patients had non-lateralized tinnitus, they were older and none had any depressive symptoms. The studies varied also in the duration and age of onset of tinnitus in the patients. Technical differences were related to the types of scanner (3 T in our study and 1.5 T in the other studies) and the MRI sequences used. We corrected for global volume in our analysis, whereas the other two studies did not. Notwithstanding these reasons, it is possible that the inherent heterogeneity of the tinnitus population may be one reason for the different results. Note also that in all three studies, alterations to the regions in the central auditory system were identified only via a constrained ROI analysis and not through the unbiased whole-brain analysis. This result points to a limitation of the technique and analytical method in estimating differences in gray matter structures in the central auditory processing pathway. Changes in small structures in the central auditory pathway are nullified by multiple comparison correction and a targeted ROI analysis becomes necessary. A meta-analysis of several VBM studies may be required to identify gray matter alterations uniquely due to tinnitus.

In addition to the subcallosal frontal cortex, we found decreases in the gray matter in dorsomedial frontal gyrus and the anterior cingulate for the NH>HL contrast. We interpret the decreases in gray matter in dorsomedial frontal gyrus and anterior cingulate as being part of the attentional and paralimbic network that is altered by hearing loss, with perhaps functional changes due to enhanced usage of the more general cognitive areas resulting in loss of gray matter. In a recent structural MRI study, Wong et al. (2010) found decreases in volume and thickness of dorsolateral prefrontal cortex in older hearing impaired adults that were associated with decreased performance on speech-in-noise tests relative to normal hearing younger adults. We also found decreases in the dorsomedial frontal gyrus, and superior frontal gyrus for the TIN>HL contrast. This suggests that there may be decreased use of the attentional network in tinnitus relative to hearing loss alone, in order to ignore the internal sound, which in turn may better preserve the gray matter in the frontal cortex. Functional brain imaging (Andersson et al., 2000; Mirz et al., 2000a,b; Weisz et al., 2004) studies of tinnitus have identified the frontal cortex as being part of the network subserving tinnitus and possibly associated with attention and emotion underlying chronic tinnitus. However, the specific role of the frontal cortex in mediating tinnitus or other activities in the presence of tinnitus remains to be elucidated. Results of both comparisons (NH>HL and TIN>HL) point to the fact that areas concerned with higher-level cognition are affected by peripheral hearing loss not associated with tinnitus.

As in the frontal cortex, we found gray matter decreases in the posterior superior temporal gyrus in both hemispheres for the hearing loss group compared to either the tinnitus group or the normal hearing group. It is surprising that hearing loss alone resulted in greater alterations of the superior temporal

cortex rather than hearing loss associated with tinnitus. Earlier functional imaging studies have shown abnormal activity in these regions in tinnitus groups compared to normal hearing control groups (Andersson et al., 2000; Mirz et al., 2000a,b; Weisz et al., 2004).

Where we found differences amongst the groups was in comparing the HL group with either the TIN or the NH group. The pattern of differences was similar in both contrasts, suggesting that hearing loss by itself causes loss of gray matter, but with the additional condition of tinnitus, there was decreased loss or better preservation of gray matter. Our results suggest that tinnitus may mask changes due to hearing loss, in other words, sensory deprivation results in loss of gray matter, but perception of an internal sound (tinnitus) may moderate this loss. However, this speculation requires further empirical support.

3.2. DTI

In the DTI analysis, the most significant changes due to hearing loss occurred in the right anterior thalamic radiation which projects out of the anterior and medial regions of the thalamus (Wakana et al., 2004) and via the internal capsule connects with the frontal lobe. A specific portion of the anterior thalamic radiation, the acoustic radiation, is a fiber tract originating in the medial geniculate nucleus and terminating in primary auditory cortex or Heschl's gyrus. We also found changes in orientation of the superior and inferior longitudinal fasciculi, corona radiata, anterior thalamic tract, and the fronto-occipital tract, all in the right hemisphere. Unlike Lin et al. (2008) and Wu et al. (2009) we did not find any changes in the subcortical pathways of the lateral lemniscus or those via the inferior colliculus in both hearing loss groups. Our finding of decreased FA values in the tracts of the internal capsule, superior longitudinal fasciculus and nerve fibers of the of the frontal pathways is similar to the such findings in early deaf individuals when compared to normal hearing controls (Kim et al., 2009). Such plastic changes could be due to, among other reasons, sensory deprivation or compensatory mechanisms resulting in either damage to white matter tracts (axonal loss or demyelination) or more disordered white matter caused by expansion of other fibers into the region. The superior longitudinal fasciculus, also called the arcuate fasciculus, connects the fronto-temporal and fronto-parietal regions (Catani et al., 2002). The inferior longitudinal fasciculus connects the ipsilateral temporal and occipital lobes (Catani et al., 2002). Its main function, similar to that of the superior longitudinal fasciculus, appears to be integration of information between the speech and auditory regions in the cortex. Fiber bundles leading to and from the cortex pass through the corona radiata that connects onto the internal capsule. The corticospinal tract originates from the pyramidal cells in the premotor, motor and sensory cortex and descends to the spinal cord. It forms the posterior limb of the internal capsule and its primary function is in voluntary activity. The superior fronto-occipital tract connects the frontal lobe to the ipsilateral parietal lobe. The inferior fronto-occipital tract connects the ipsilateral frontal and occipital lobes, ipsilateral frontal and posterior parietal and temporal lobes and mixes with the uncinate fasciculus (Catani et al., 2002). Its primary function

is integration of auditory and visual association areas with prefrontal cortex.

3.3. Combined VBM and DTI

Our study used multimodal imaging to inspect both white and gray matter changes related to hearing loss or chronic tinnitus. A recent paper (Giorgio et al., 2010) similarly investigated gray and white matter changes occurring with age throughout adulthood. The study found widespread reductions in gray matter with age, with the earliest reductions occurring in the frontal cortex. This is similar to our finding of hearing loss-related reductions in gray matter in the frontal cortex in older adults. Although our study had age-matched controls and did not seek to investigate age-related changes, it is possible that age-related changes in the frontal cortex occur earlier in those with hearing loss. Giorgio et al. (2010) analyzed changes in white matter using both DTI and volume estimates by VBM. They found that DTI-based markers were earlier detectors of white matter changes than volume estimates of VBM. In our study, we used only DTI-based FA measures, and we found that reduced FA values in the anterior thalamic radiation, inferior fronto-occipital tract and superior and inferior longitudinal fasciculus in the right hemisphere, were related to hearing loss. Similarly, the Giorgio study found declines mostly in the right hemisphere, for the anterior thalamic radiation and superior longitudinal fasciculus (among other tracts) using volumetric methods and in the right corona radiata using DTI measures. Age-related declines in gray and white matter may be associated with hearing loss. Prevalence of hearing loss increases with age, with approximately one in three individuals above the age of 65 and one in two individuals above the age of 75 suffer from some hearing impairment (Davis, 1994, 1989). The Giorgio study did not report on the hearing status of their participants; it is possible that some may have been hearing impaired. A systematic study incorporating both age and hearing loss as factors is needed to tease apart the contributions of these factors on white and gray matter changes.

Both hearing loss and tinnitus cause neuroplastic changes in the brain; however, the type, degree, and location of such changes vary. Some researchers hold that tinnitus itself, may be a result of neuroplasticity occurring due to hearing loss (for a review, see Moller, 2006). In our study, we found distinct patterns of gray and white matter changes in hearing loss and tinnitus with respect to age-matched normal hearing controls. The greatest changes (relative to normal hearing controls) were in participants with hearing loss alone and not as expected, in those with hearing loss and tinnitus. This result however, does not preclude more profound functional changes occurring for those with hearing loss and tinnitus relative to those with hearing loss alone. Several imaging studies have shown changes associated with tinnitus in large-scale functional networks encompassing both cortical and subcortical regions (Giraud et al., 1999; Lockwood et al., 1998; Lockwood et al., 2001; Mirz et al., 1999, 2000a; Schlee et al., 2008). In the visual modality, studies have shown distinct patterns of structural changes in the occipital cortex associated with sensory deprivation in the case of macular degeneration or glaucoma (Boucard et al., 2009) compared to

the condition of persistent visual disturbances caused by migraine (similar to intermittent tinnitus) (Jager et al., 2005). Boucard et al. (2009) found gray matter declines in retinal lesion projection zones of the visual cortex for both foveal (related to macular degeneration) and peripheral (related to glaucoma) retinal lesions. Gray matter reductions in both visual and non-visual (parietal-occipital and ventral temporal) cortices were found in children with amblyopia, whereas adults primarily had decreases in the visual cortex (Mendola et al., 2005). In contrast, Jager et al. (2005) did not find any regional changes in water diffusion along white matter tracts in either the visual or non-visual cortices in patients suffering from persistent visual disturbances.

Our results show that the interaction between hearing loss and tinnitus is more complicated than an additive effect of tinnitus on a baseline hearing impaired condition. One interpretation of the study results would be that a subset of those with hearing impairment (those who happen to have tinnitus) do not show gray matter declines and reduced white matter integrity to the extent of another sub-group relative to normal hearing controls. Another interpretation would be that generation and perception of persistent internal noise and related functional mechanisms that allow the individual to compensate for the noise may offset changes related to sensory deprivation.

Our study had a number of limitations. First, the small number of subjects in the three groups might have underpowered the comparison analyses. However, there have been other VBM studies with small number of patients (Kubicki et al., 2002; Salgado-Pineda et al., 2003; Trivedi et al., 2006). To counteract type I errors affecting our results due to small n , we used a mask of the ANOVA results to filter the post-hoc group VBM results. For ROI analysis, we used *a priori* hypotheses about hearing impairment and tinnitus affecting auditory processing regions and previously published mask to constrain our analysis. DTI studies may also be conducted with small number of subjects. For instance, the Chang et al. (2004) study had 10 patients with sensorineural hearing loss and 10 controls with normal hearing. We found statistically significant changes in the HL vs. NH comparisons for both VBM and DTI analyses, strengthening our conclusions. Further, both analyses point to structural changes near the auditory cortex to a greater extent for the hearing loss group relative to those with tinnitus and hearing loss or the control group. Second, we could not test for changes occurring with time within a group—the design was cross-sectional and not longitudinal. A longitudinal study will be better at first detection of changes due to hearing loss or chronic tinnitus. Further, some of the changes seen in our study may be due to age (the participants in our study had a mean age in the mid-fifties). Although the control subjects were age-matched to the patient groups, some of the age-related changes may appear earlier in the hearing loss group relative to the other groups. We also cannot definitively claim that hearing loss causes these changes. The between-group differences seen here are suggestive of causality but could be due to pre-existing anatomical differences. A larger study is necessary to dissociate the effects of age from those of hearing loss alone.

In conclusion, our study found that the condition of sensorineural hearing loss causes changes in the gray matter

volume in the superior temporal cortex and the white matter tracts near auditory cortex, in the temporal cortex. There were also changes in the volume of gray matter and orientation of white matter in distal regions that are connected to the auditory cortex. Such combined changes in both white and gray matter may be due to sensory deprivation or compensatory plasticity. When we compared individuals with hearing loss coupled and chronic tinnitus to normal hearing controls without tinnitus, there was no statistically significant change in gray matter volume or orientation of white matter tracts. There may be an association between the chronic perception of an internal noise and less severe changes in neural tissue in the event of hearing loss. Further studies, combining functional and structural imaging related to hearing loss or tinnitus, are necessary to expand on the present results.

4. Experimental procedures

4.1. Subjects

All participants understood and signed a written consent for NIH/NINDS-NIDCD IRB Protocol 06-DC-0218 and were suitably compensated. They were recruited from the greater Washington, D.C. metropolitan area.

The tinnitus group (TIN) consisted of 8 male volunteers (age range=42–64 years, mean=56.13 years, SD=7.04 years) with bilateral, mild-to-moderate hearing loss and chronic subjective tinnitus that had persisted for between 3 and 38 years at the time of their scan. The tinnitus percept was most frequently described as a buzzing, ringing, hissing or whistle. Others described a hum, clear tone or pulsating percept (all subjects denied changes in time with heartbeat or respiration). One subject perceived the sound of cicadas. Five subjects described more than one of the above sounds. Tinnitus severity was evaluated by the Tinnitus Handicap Inventory and all subjects were either grade 1 – slight or grade 2 – mild (range=10–26, mean=17.25, SD=5.01) (McCombe et al., 2001; Newman et al., 1996). Six subjects experienced their tinnitus bilaterally or in the “middle of the head.” Two subjects described their tinnitus as more left lateralized but still central. Of the 28 (6 female) individuals with tinnitus screened for this study, only 8 male patients met our criteria for symmetrical high-frequency sensorineural hearing loss and chronic tinnitus. The others were not included in the study due to our stringent exclusionary criteria of the type of hearing loss, type of tinnitus, and other physical or mental health issues.

The second group (HL) ($n=7$) was matched in age (age range=31–64 years, mean=51.38 years, SD=11.45 years), gender and hearing loss and only had bilateral, mild-to-moderate hearing loss with no tinnitus. The third group (NH) ($n=11$) was age (age range=32–63 years, mean=48.09 years, SD=10.42 years) and gender-matched and had normal hearing with no tinnitus. All subjects scored in the minimal depression range on the Beck Depression Inventory (BDI-II) (range=0–10, mean for TIN=1.45, mean for HL=0.57, mean for NH=0.75). After initial screening, all potential participants were evaluated by a licensed medical practitioner and were excluded if they had current, or a history of, temporomandibular joint problems, hyperacusis, Meniere's

disease, benign positional vertigo or any other health issues that may have presented complications or contraindications with MRI. Data from 3 normal hearing volunteers and 1 participant with tinnitus were not included in the DTI analysis due to excessive head motion in their diffusion images.

4.2. Audiometric evaluation

All included subjects underwent full audiometric evaluation before and after the scanning session at the NIH Clinical Center Otolaryngology clinic in a double-walled audiometric booth using a GSI 61 audiometer and ER-3A transducer. This included single frequency (226 Hz) tympanometry, distortion product otoacoustic emissions measured in quarter octave bands from 842 to 7996 Hz, spontaneous otoacoustic emission testing, speech and pure tone, air conduction audiometry at 250, 500, 1000, 2000, 3000, 4000, 6000 and 8000 Hz, loudness tolerance evaluation using pre-recorded MRI scanner sounds, acoustic reflex and reflex decay testing. All subjects had normal hearing (defined as hearing loss of no more than 25 dB HL at any of the 8 frequencies tested between 250 and 8000 Hz) up to 2000 Hz. NH subjects had normal hearing at all additional frequencies while TIN and HL subjects had moderate to moderately severe hearing loss (no greater than 70 dB as defined by Clark, 1981, and noted at <http://www.asha.org/public/hearing/disorders/types.htm>) for the testing frequencies from 2000 to 8000 Hz. The hearing loss of all groups is summarized in Table 1. There were no statistically significant differences in the pure tone average hearing loss (across all testing frequencies) ($p=0.89$ using Wilcoxon rank sum test) or at the higher frequencies (4, 6, 8 kHz) ($p=0.69$ using Wilcoxon rank sum test) for the TIN and HL groups.

4.3. Data acquisition

Participants were scanned in a 3 T GE Excite scanner using an eight-channel receive-only coil.

4.3.1. VBM

Imaging parameters for the 3D-FSPGR (3 dimensional fast spoiled gradient-recalled acquisition in a steady-state) sequences were: 128 slices; field of view, 24 mm; repetition time, 30 ms; resolution, $0.9375 \times 0.9375 \times 1.3$ mm, flip angle, 12° . The scans were screened by a neuroradiologist for abnormalities; none were found in the participants described in the present study.

4.3.2. DTI

The DTI sequence for whole-brain coverage used a single-shot spin-echo echo-planar imaging sequence with paired gradient pulses positioned 180° around the refocusing pulse for diffusion weighting and sensitivity-encoding (ASSET) for rate 2 acceleration. Imaging parameters for the diffusion-weighted sequence were TE/TR=73.4/13 000 ms, FOV= 2.4×2.4 cm²; matrix= 96×96 mm² zero-filled to 256×256 mm²; 54 contiguous axial slices with slice thickness of 2.4 mm. Diffusion was measured along 33 non-collinear directions with a b factor of 1000 s/mm². Three reference images were acquired with no

diffusion gradients applied (b_0 scans). The same acquisition sequence was repeated twice.

4.4. Data processing and statistical analysis

4.4.1. VBM

Statistical parametric software (SPM5, Wellcome Trust Centre for Neuroimaging, <http://www.fil.ion.ucl.ac.uk/spm/software/spm5/>) was used to analyze the data. We preprocessed each subject's structural MRI scan by means of a modified optimized-VBM-protocol as previously described by Good et al. (2001) involving normalization, optional modulation, segmentation, and smoothing. We did not create customized study specific prior probability maps for reducing scanner specific bias; instead, we employed a single generative model defined as unified segmentation (Ashburner and Friston, 2005). Unified segmentation incorporates the processes of normalization, modulation, and segmentation. It allows for variation in image intensity among scans by estimating tissue class intensities from spatial priors suited to the image, and includes the scanner bias correction of the optimized-VBM-protocol in its algorithm. In this process, all the scans were standardized to the same anatomical space and segmented either as modulated or unmodulated images. SPM5 uses a 12-parameter affine transformation, and then applies nonlinear deformations to normalize the images onto the stereotactic space (152 T1 MNI template, Montreal Neurological Institute). In warping each brain image during normalization, certain regions of the brain suffer either a volumetric growing or shrinking effect. This does not affect identification of regional differences in the concentration of gray matter (Ashburner and Friston, 2000). However, in order to preserve the actual amounts of gray matter (volume) within each structure, an additional correctional procedure known as modulation is typically applied. Modulation involves the multiplication of the partitioned images by the relative voxel volumes, or Jacobian determinants of the deformation field (Ashburner and Friston, 2000). Following normalization and optional modulation, the scans were segmented to differentiate gray matter from white matter and cerebrospinal fluid through a modified mixture model cluster analysis technique (Ashburner and Friston, 2000). Compensating for the effects of spatial normalization has critical implications for the interpretation of VBM data. Unmodulated VBM data facilitate comparison of relative concentration of gray or white matter in spatially normalized images. Modulated VBM data allow us to determine absolute volume of gray or white matter structures (Mechelli et al., 2005). Thus, we obtained two gray matter images for each subject: modulated images to detect differences in volume of gray matter, and unmodulated images to identify discrepancies in regional concentration of gray matter between populations. We did not analyze white matter size in this study. Image intensity non-uniformity was accounted for during segmentation (Ashburner and Friston, 2000; Ashburner and Friston, 2005). We then applied an isotropic smoothing Gaussian kernel of 8 mm full width at half maximum (FWHM) to the images. This low pass filter reduces signal noise and artifacts that could be present due to head

movement during MRI acquisition and residual inter-subject variability introduced by normalization.

We performed both whole-brain and region-of-interest (ROI) VBM analyses, each of which provide somewhat different information. Whole-brain analysis is automated and un-biased, making no assumptions of about any regions of particular interest. However, this technique requires a great number of subjects to achieve statistical significance and it is possible that changes in smaller structures (for instance, inferior colliculus) may not be easily identified. This is one of the reasons why it is common practice to conduct a secondary region-of-interest analysis, testing for statistically significant differences only in the voxels that are deemed of interest by an *a priori* hypothesis. An ROI analysis can be used to corroborate the findings of previous studies, or those obtained during the whole-brain analysis. This is of special importance in studies with a small sample size.

4.5. Unbiased whole-brain analysis

Statistical analysis was performed on the gray matter images using a general linear model. We considered both modulated and unmodulated data for this study because the former describes changes in volume and the latter in concentration of gray matter. We corrected for differences in total brain volume by incorporating total intracranial volume (TIV) as a covariate in our multiple regression analysis. A one-way analysis of variance (ANOVA) for testing the equality of means among our three populations was used to determine the main effect of group on gray matter. We then performed two-sample *t* tests masked by the ANOVA main effects results to evaluate (1) HL vs. NH, (2) TIN vs. HL, and (3) TIN vs. NH and masked the results. We performed these tests on a voxel-by-voxel basis, excluding all voxels with gray matter value less than 0.2 to avoid possible edge effects around the border between white and gray matter and to include only voxels with sufficient gray matter. We accounted for heterogeneity of variance among the groups by using the non-sphericity correction. For the whole-brain analysis, we set the significance at $p < .001$ uncorrected at the voxel-level and $p < 0.05$ family-wise error (FWE) and false discovery rate (FDR) corrected at the cluster level for multiple comparisons and used an extent threshold of 50 contiguous voxels. Apart from the conventional parametric approach based on Gaussian field theory outlined here, we performed a separate non-parametric analysis. The statistical non-parametric analysis (SnPM; (Nichols and Holmes, 2002), <http://www.sph.umich.edu/ni-stat/SnPM/>) does not assume a normally distributed data set, which is especially pertinent due to our small sample size.

4.6. Region-of-interest analysis

For the ROI analysis, we used a mask of cortical and subcortical regions in the central auditory system previously used by Muhlau et al. (2006) and Landgrebe et al. (2009). In order to maintain compatibility of our results with both of these published studies, we used the same anatomical mask wherein the ROI encompassed the ventral and dorsal cochlear nuclei (sphere radius, 5 mm; Montreal Neurological Institute (MNI) coordinates, $\pm 10, -38, -45$), the superior olivary complex (sphere radius, 5 mm; MNI coordinates, $\pm 13, -35, -41$), the inferior

colliculus (sphere radius, 5 mm; MNI coordinates, $\pm 6, -33, -11$), and the medial geniculate nucleus (MGN) (sphere radius, 8 mm; MNI coordinates, $\pm 17, -24, -2$), as well as the primary and secondary auditory cortices corresponding to Brodmann areas 41, 42, and 22 (defined in MNI coordinate space with the WFU-Pickatlas; Maldjian et al., 2003). The main advantage of using a *a priori* ROI testing over whole-brain analysis is that it limits type I error by reducing the number of statistical tests to only a few ROIs. These tests were conducted at an exploratory significance of $p < 0.005$ uncorrected, with an extent threshold of 20 voxels.

Next, we ran a multiple regression analysis to test for any association between hearing loss and changes in gray matter. We used a combined mask of the auditory pathway ROIs and significant clusters from the whole-brain ANOVA analysis and incorporated the pure tone average values at 2, 4, 6, and 8 kHz. We chose these frequency values because they directly assessed the extent of hearing loss of our participants. We set the statistical significance of this second ROI analysis at $p < 0.001$ uncorrected, and $p < 0.05$ false discovery rate (FDR) corrected at the voxel-level and the minimum contiguous cluster size at 50 voxels. Using a previously defined anatomical mask prevented the finding of spurious correlations between behavioral measures and imaging markers (Vul et al., 2009).

4.6.1. DTI

We prepared the FA images using MRICron's (<http://www.cabiatl.com/micro/mricron/index.html>) dcm2nifti tool and FMRIB Software Library (FSL, <http://www.fmrib.ox.ac.uk/fsl/>). After acquiring the necessary diffusion-weighted data, the DTI images of each subject were registered with FSL (FMRIB Software Library, Smith et al., 2004), and the related FMRIB's Diffusion toolbox (Behrens et al., 2003). After the image conversion, the images were prepared by merging two separate DTI runs for each subject. The images were corrected for eddy-currents and motion artifacts by running eddy-correction and aligning all volumes to the first weighted volume for each subject (FLIRT in FSL). A skull stripping procedure (Brain Extraction Tool in FSL) was employed on all images to generate a mask that excluded non-brain tissue. In order to create the final FA image, DTIFIT takes the masked, eddy-corrected DTI data, and defines a diffusion tensor model for each voxel. The diffusion tensor was characterized by eigenvalues and eigenvectors that describe the quality and directionality of each tensor. DTIFIT created three 3D image maps based on the eigenvalues and eigenvectors, one for FA values, one for mean diffusivity values, and another which reported the mode of anisotropy for each voxel. We only report on the FA values obtained for the participants of each of the three groups.

FA images were created by fitting a tensor model to the raw diffusion data using FDT, and then brain-extracted using Brain Extraction Tool (Smith, 2002). The FA data were then aligned into a common space using the nonlinear registration tool FNIRT (FMRIB's nonlinear image registration tool) (Andersson et al., 2007a,b), which uses a *b*-spline representation of the registration warp field (Rueckert et al., 1999). The mean FA image was created and transformed into a mean FA skeleton that characterizes the centers of all tracts common to the group. Each subject's aligned FA data was then projected onto this skeleton and the resulting data fed into voxel-wise cross-subject statistics.

4.7. Unbiased whole-brain analysis

For reasons detailed in the previous VBM section, we performed both whole-brain and ROI analyses of DTI data. Voxel-wise statistical analysis of the FA data was carried out using TBSS (Tract-Based Spatial Statistics, Smith et al., 2006, part of FSL, Smith et al., 2004). The technique allows the application of voxel-wise cross-subject statistics by projecting all subjects' FA data onto a mean FA tract skeleton. TBSS was used to identify differences in white matter tracts among the three subject groups. The FA images of each subject were registered to a reference image, which in this case was the image of the 'most typical' subject. After the images were aligned to each other, they were placed in a standard space and an FA skeleton was created. After this alignment, which creates a mean FA skeleton, all of the images were projected onto this mean skeleton and thresholded at 0.2, which allowed for the inclusion of large white matter pathways and exclusion of smaller peripheral tracts that may be variable among the participants. Statistical analyses for each point of the FA skeleton were conducted using FSL statistic modelling program, *randomise*, to test for significant differences between each pair of groups using a permutation-based method (Freedman and Lane, 1983; Hayasaka and Nichols, 2003). Permutation tests belong to the family of non-parametric tests and do not make assumptions about the underlying probability distribution. Correction for multiple comparisons was performed using threshold-free cluster enhancement (tcf) process that is more robust than a cluster-based thresholding technique because it does not begin with an arbitrary cluster-forming threshold. For the group comparisons we used two-sample *t* tests with a significance level of $p < 0.1$, corrected for multiple comparisons. To examine the effect of hearing loss we performed a multiple regression analysis with PTA hearing loss values at 2, 4, 6, and 8 kHz as a covariate. We did this only for the NH>HL contrast because this comparison produced suprathreshold clusters. We again used a threshold of $p < 0.1$ corrected for multiple comparisons. To enhance pictorial depiction, we used *tbss_fill* procedure to fill out the significant tracts.

4.8. Region-of-interest analysis

We performed a region-of-interest (ROI) analysis to further examine differences between the three groups. We defined the ROI as the region which exhibited the largest FA value differences between the NH and HL groups in the whole-brain and regression with PTA analysis. The ROI was drawn as an ellipsoid centered at [31, -37, 16] (with axes $a=2$, $b=5$, $c=2$) that includes tracts from the anterior thalamic radiation, inferior longitudinal fasciculus and inferior fronto-occipital fasciculus and borders superior longitudinal fasciculus. We used an uncorrected threshold of $p < 0.05$ in order to include all voxels in the ROI for all three groups. Fig. 5b shows the uncorrected NH>HL results at $z=17$ and the ROI drawn on the right hemisphere. An ROI mask was applied to each individual's FA skeleton image that had previously been nonlinearly aligned to the MNI standard image. The mean FA intensity value was calculated for each subject over this mask, and zero-intensity voxels that were not part of the white matter were excluded. While the hearing loss was bilateral, the ROI in the left hemisphere did not show significant differences in FA values,

therefore we only report the results from the right hemisphere (Fig. 5c). In Fig. 5c, we plot the FA values for this ROI for each participant against their PTA hearing loss estimates at 2, 4, 6, and 8 kHz.

Acknowledgments

The research was supported by the NIH-NIDCD Intramural Research Program and a grant from the Tinnitus Research Consortium to FTH. We are grateful to Dr. Allen Braun of the Language Section and the Audiology clinic staff of NIDCD-NIH: Dr. H. J. Kim, Dr. C. Brewer, Nurse Practitioner S. Rudy, audiologist C. Zalewski, for their diligent efforts in screening the participants in the study. We thank Kathy Xu for her help in the initial stages of the DTI analysis and Christopher Grindrod for his comments on earlier drafts of this manuscript.

REFERENCES

- Adams, P.F., Hendershot, G.E., Marano, M.A., 1999. Current estimates from the National Health Interview Survey, 1996. *Vital. Health. Stat.* 10, 1–203.
- Andersson, G., Lyttkens, L., Hirvela, C., Furmark, T., Tillfors, M., Fredrikson, M., 2000. Regional cerebral blood flow during tinnitus: a PET case study with lidocaine and auditory stimulation. *Acta Otolaryngol.* 120, 967–972.
- Andersson, J.L.R., Jenkinson, M., Smith, S., 2007a. Non-linear registration, aka spatial normalisation. FMRIB technical report. Vol. TR07JA2.
- Andersson, J.L.R., Jenkinson, M., Smith, S., 2007b. Non-linear optimisation. FMRIB technical report. Vol. TR07JA1.
- Ashburner, J., Friston, K.J., 2000. Voxel-based morphometry—the methods. *Neuroimage* 11, 805–821.
- Ashburner, J., Friston, K.J., 2005. Unified segmentation. *Neuroimage* 26, 839–851.
- Barnea, G., Attias, J., Gold, S., Shahar, A., 1990. Tinnitus with normal hearing sensitivity: extended high-frequency audiometry and auditory-nerve brain-stem-evoked responses. *Audiology* 29, 36–45.
- Basta, D., Tzschentke, B., Ernst, A., 2005. Noise-induced cell death in the mouse medial geniculate body and primary auditory cortex. *Neurosci. Lett.* 381, 199–204.
- Basta, D., Goetze, R., Ernst, A., 2008. Effects of salicylate application on the spontaneous activity in brain slices of the mouse cochlear nucleus, medial geniculate body and primary auditory cortex. *Hear. Res.* 240, 42–51.
- Behrens, T.E., Woolrich, M.W., Jenkinson, M., Johansen-Berg, H., Nunes, R.G., Clare, S., Matthews, P.M., Brady, J.M., Smith, S.M., 2003. Characterization and propagation of uncertainty in diffusion-weighted MR imaging. *Magn. Reson. Med.* 50, 1077–1088.
- Boucard, C.C., Hernowo, A.T., Maguire, R.P., Jansonius, N.M., Roerdink, J.B., Hooymans, J.M., Cornelissen, F.W., 2009. Changes in cortical grey matter density associated with long-standing retinal visual field defects. *Brain* 132, 1898–1906.
- Catani, M., Howard, R., Pajevic, S., Jones, D., 2002. Virtual in vivo interactive dissection of white matter fasciculi in the human brain. *Neuroimage* 17, 77–94.
- Chang, Y., Lee, S.H., Lee, Y.J., Hwang, M.J., Bae, S.J., Kim, M.N., Lee, J., Woo, S., Lee, H., Kang, D.S., 2004. Auditory neural pathway evaluation on sensorineural hearing loss using diffusion tensor imaging. *NeuroReport* 15, 1699–1703.

- Chen, G.D., Jastreboff, P.J., 1995. Salicylate-induced abnormal activity in the inferior colliculus of rats. *Hear. Res.* 82, 158–178.
- Clark, J.G., 1981. Uses and abuses of hearing loss classification. *ASHA* 23, 493–500.
- Davis, A., 1994. Prevalence of hearing impairment. In: Davis, A. (Ed.), *Hearing in Adults*. Whurr Publishers Ltd., London, pp. 43–321.
- Davis, A., Razaie, E.A., 2000. Epidemiology of tinnitus. In: Tyler, R.S. (Ed.), *Tinnitus Handbook*. Singular, San Diego, CA.
- Davis, A.C., 1989. The prevalence of hearing impairment and reported hearing disability among adults in Great Britain. *Int. J. Epidemiol.* 18, 911–917.
- Eggermont, J.J., Kenmochi, M., 1998. Salicylate and quinine selectively increase spontaneous firing rates in secondary auditory cortex. *Hear. Res.* 117, 149–160.
- Freedman, D.A., Lane, D., 1983. A nonstochastic interpretation of reported significance levels. *J. Bus. Econ. Statist.* 1, 292–298.
- Giorgio, A., Santelli, L., Tomassini, V., Bosnell, R., Smith, S., De Stefano, N., Johansen-Berg, H., 2010. Age-related changes in grey and white matter structure throughout adulthood. *Neuroimage* 51, 943–951.
- Giraud, A.L., Chery-Croze, S., Fischer, G., Fischer, C., Vighetto, A., Gregoire, M.C., Lavenne, F., Collet, L., 1999. A selective imaging of tinnitus. *NeuroReport* 10, 1–5.
- Good, C.D., Johnsrude, I.S., Ashburner, J., Henson, R.N., Friston, K.J., Frackowiak, R.S., 2001. A voxel-based morphometric study of ageing in 465 normal adult human brains. *Neuroimage* 14, 21–36.
- Hayasaka, S., Nichols, T.E., 2003. Validating cluster size inference: random field and permutation methods. *Neuroimage* 20, 2343–2356.
- Jager, H.R., Giffin, N.J., Goadsby, P.J., 2005. Diffusion- and perfusion-weighted MR imaging in persistent migrainous visual disturbances. *Cephalalgia* 25, 323–332.
- Kaltenbach, J.A., Zhang, J., Afman, C.E., 2000. Plasticity of spontaneous neural activity in the dorsal cochlear nucleus after intense sound exposure. *Hear. Res.* 147, 282–292.
- Kim, D.J., Park, S.Y., Kim, J., Lee, D.H., Park, H.J., 2009. Alterations of white matter diffusion anisotropy in early deafness. *NeuroReport* 20, 1032–1036.
- Kim, J., Morest, D.K., Bohne, B.A., 1997. Degeneration of axons in the brainstem of the chinchilla after auditory overstimulation. *Hear. Res.* 103, 169–191.
- Kubicki, M., Shenton, M.E., Salisbury, D.F., Hirayasu, Y., Kasai, K., Kikinis, R., Jolesz, F.A., McCarley, R.W., 2002. Voxel-based morphometric analysis of gray matter in first episode schizophrenia. *Neuroimage* 17, 1711–1719.
- Landgrebe, M., Langguth, B., Rosengarth, K., Braun, S., Koch, A., Kleinjung, T., May, A., de Ridder, D., Hajak, G., 2009. Structural brain changes in tinnitus: grey matter decrease in auditory and non-auditory brain areas. *Neuroimage* 46, 213–218.
- Lee, S.H., Chang, Y., Lee, J.E., Cho, J.H., 2004. The values of diffusion tensor imaging and functional MRI in evaluating profound sensorineural hearing loss. *Cochlear Implants Int.* 5 (Suppl 1), 149–152.
- Lee, Y.J., Bae, S.J., Lee, S.H., Lee, J.J., Lee, K.Y., Kim, M.N., Kim, Y.S., Baik, S.K., Woo, S., Chang, Y., 2007. Evaluation of white matter structures in patients with tinnitus using diffusion tensor imaging. *J. Clin. Neurosci.* 14, 515–519.
- Lin, Y., Wang, J., Wu, C., Wai, Y., Yu, J., Ng, S., 2008. Diffusion tensor imaging of the auditory pathway in sensorineural hearing loss: changes in radial diffusivity and diffusion anisotropy. *J. Magn. Reson. Imaging* 28, 598–603.
- Lockwood, A.H., Salvi, R.J., Coad, M.L., Towsley, M.L., Wack, D.S., Murphy, B.W., 1998. The functional neuroanatomy of tinnitus: evidence for limbic system links and neural plasticity. *Neurology* 50, 114–120.
- Lockwood, A.H., Wack, D.S., Burkard, R.F., Coad, M.L., Reyes, S.A., Arnold, S.A., Salvi, R.J., 2001. The functional anatomy of gaze-evoked tinnitus and sustained lateral gaze. *Neurology* 56, 472–480.
- Lockwood, A.H., Salvi, R.J., Burkard, R.F., 2002. Tinnitus. *N Engl J. Med.* 347, 904–910.
- Maldjian, J.A., Laurienti, P.J., Kraft, R.A., Burdette, J.H., 2003. An automated method for neuroanatomic and cytoarchitectonic atlas-based interrogation of fMRI data sets. *Neuroimage* 19, 1233–1239.
- McCombe, A., Baguley, D., Coles, R., McKenna, L., McKinney, C., Windle-Taylor, P., 2001. Guidelines for the grading of tinnitus severity: the results of a working group commissioned by the British Association of Otolaryngologists, Head and Neck Surgeons, 1999. *Clin. Otolaryngol. Allied Sci.* 26, 388–393.
- Mechelli, A., Price, C.J., Friston, K.J., Ashburner, J., 2005. Voxel-based morphometry of the human brain: methods and applications. *Curr. Med. Imaging Rev.* 1, 105–113.
- Mendola, J.D., Conner, I.P., Roy, A., Chan, S.T., Schwartz, T.L., Odom, J.V., Kwong, K.K., 2005. Voxel-based analysis of MRI detects abnormal visual cortex in children and adults with amblyopia. *Hum. Brain Mapp.* 25, 222–236.
- Mirz, F., Pedersen, B., Ishizu, K., Johannsen, P., Ovesen, T., Stodkilde-Jorgensen, H., Gjedde, A., 1999. Positron emission tomography of cortical centers of tinnitus. *Hear. Res.* 134, 133–144.
- Mirz, F., Gjedde, A., Ishizu, K., Pedersen, C.B., 2000a. Cortical networks subserving the perception of tinnitus—a PET study. *Acta Otolaryngol. Suppl.* 543, 241–243.
- Mirz, F., Gjedde, A., Stodkilde-Jrgensen, H., Pedersen, C.B., 2000b. Functional brain imaging of tinnitus-like perception induced by aversive auditory stimuli. *NeuroReport* 11, 633–637.
- Moller, A.R., 2006. Neural plasticity in tinnitus. *Prog. Brain Res.* 157, 365–372.
- Moller, A.R., 2007. Tinnitus: presence and future. *Prog. Brain Res.* 166, 3–16.
- Muhlau, M., Rauschecker, J.P., Oestreicher, E., Gaser, C., Rottinger, M., Wohlschlagel, A.M., Simon, F., Etgen, T., Conrad, B., Sander, D., 2006. Structural brain changes in tinnitus. *Cereb. Cortex* 16, 1283–1288.
- Newman, C.W., Jacobson, G.P., Spitzer, J.B., 1996. Development of the tinnitus handicap inventory. *Arch. Otolaryngol. Head Neck Surg.* 122, 143–148.
- Nichols, T.E., Holmes, A.P., 2002. Nonparametric permutation tests for functional neuroimaging: a primer with examples. *Hum. Brain Mapp.* 15, 1–25.
- Penhune, V.B., Cismaru, R., Dorsaint-Pierre, R., Petitto, L.A., Zatorre, R.J., 2003. The morphometry of auditory cortex in the congenitally deaf measured using MRI. *Neuroimage* 20, 1215–1225.
- Rueckert, D., Sonoda, L.I., Hayes, C., Hill, D.L., Leach, M.O., Hawkes, D.J., 1999. Nonrigid registration using free-form deformations: application to breast MR images. *IEEE Trans. Med. Imaging* 18, 712–721.
- Salgado-Pineda, P., Baeza, I., Perez-Gomez, M., Vendrell, P., Junque, C., Bargallo, N., Bernardo, M., 2003. Sustained attention impairment correlates to gray matter decreases in first episode neuroleptic-naive schizophrenic patients. *Neuroimage* 19, 365–375.
- Schlee, W., Weisz, N., Bertrand, O., Hartmann, T., Elbert, T., 2008. Using auditory steady state responses to outline the functional connectivity in the tinnitus brain. *PLoS ONE* 3, e3720.
- Schneider, P., Andermann, M., Wengenroth, M., Goebel, R., Flor, H., Rupp, A., Diesch, E., 2009. Reduced volume of Heschl's gyrus in tinnitus. *Neuroimage* 45, 927–939.
- Shibata, D.K., 2007. Differences in brain structure in deaf persons on MR imaging studied with voxel-based morphometry. *AJNR Am. J. Neuroradiol.* 28, 243–249.
- Smith, S.M., 2002. Fast robust automated brain extraction. *Hum. Brain Mapp.* 17, 143–155.
- Smith, S.M., Jenkinson, M., Woolrich, M.W., Beckmann, C.F., Behrens, T.E., Johansen-Berg, H., Bannister, P.R., De Luca, M., Drobnjak, I., Flitney, D.E., Niaz, R.K., Saunders, J., Vickers, J.,

- Zhang, Y., De Stefano, N., Brady, J.M., Matthews, P.M., 2004. Advances in functional and structural MR image analysis and implementation as FSL. *Neuroimage* 23 (Suppl 1), S208–S219.
- Smith, S.M., Jenkinson, M., Johansen-Berg, H., Rueckert, D., Nichols, T.E., Mackay, C.E., Watkins, K.E., Ciccarelli, O., Cader, M.Z., Matthews, P.M., Behrens, T.E., 2006. Tract-based spatial statistics: voxelwise analysis of multi-subject diffusion data. *Neuroimage* 31, 1487–1505.
- Smits, M., Kovacs, S., de Ridder, D., Peeters, R.R., van Hecke, P., Sunaert, S., 2007. Lateralization of functional magnetic resonance imaging (fMRI) activation in the auditory pathway of patients with lateralized tinnitus. *Neuroradiology* 49, 669–679.
- Trivedi, M.A., Wichmann, A.K., Torgerson, B.M., Ward, M.A., Schmitz, T.W., Ries, M.L., Kosciak, R.L., Asthana, S., Johnson, S.C., 2006. Structural MRI discriminates individuals with Mild Cognitive Impairment from age-matched controls: a combined neuropsychological and voxel based morphometry study. *Alzheimers Dement.* 2, 296–302.
- Vul, E., Harris, C., Winkielman, P., Pashler, H., 2009. Puzzlingly high correlations in fMRI studies of emotion, personality and social cognition. *Perspect. Psychol. Sci.* 4, 274–290.
- Wakana, S., Jiang, H., Nagae-Poetscher, L.M., van Zijl, P.C., Mori, S., 2004. Fiber tract-based atlas of human white matter anatomy. *Radiology* 230, 77–87.
- Wang, J., Ding, D., Salvi, R.J., 2002. Functional reorganization in chinchilla inferior colliculus associated with chronic and acute cochlear damage. *Hear. Res.* 168, 238–249.
- Weisz, N., Voss, S., Berg, P., Elbert, T., 2004. Abnormal auditory mismatch response in tinnitus sufferers with high-frequency hearing loss is associated with subjective distress level. *BMC Neurosci.* 5, 8.
- Wong, P.C., Ettliger, M., Sheppard, J.P., Gunasekera, G.M., Dhar, S., 2010. Neuroanatomical characteristics and speech perception in noise in older adults. *Ear Hear.* 31, 471–479.
- Wu, C.M., Ng, S.H., Wang, J.J., Liu, T.C., 2009. Diffusion tensor imaging of the subcortical auditory tract in subjects with congenital cochlear nerve deficiency. *AJNR Am. J. Neuroradiol.* 30, 1773–1777.